THE ANATOMICAL RECORD 303:772–789 (2020)

Cranium and Vertebral Column of Xingxiulong chengi (Dinosauria: Sauropodomorpha) from the Early Jurassic of China

YA-MING WANG,[1] TAO WANG,[2] ZHI-WEN YANG,[2] AND HAI-LU YOU [3,4,5]*

[1]The Geological Museum of China, Beijing, China
[2]Bureau of Land and Resources of Lufeng County, Lufeng, Yunnan, China
[3]Key Laboratory of Vertebrate Evolution and Human Origins, Institute of Vertebrate Paleontology and Paleoanthropology, Chinese Academy of Sciences, Beijing, China
[4]CAS Center for Excellence in Life and Paleoenvironment, Beijing, China
[5]College of Earth and Planetary Sciences, University of Chinese Academy of Sciences, Beijing, China

ABSTRACT

The Lower Jurassic Lufeng Formation in Yunnan Province of southwestern China provides one of the most abundant records of sauropodomorphs in the world. However, most of them have not been fully described. Xingxiulong chengi is among the most complete non-sauropodan sauropodomorphs ever discovered from Lufeng Formation and is represented by three partial skeletons. Here, we provide a detailed osteological description of its axial skeleton, including both the cranial and postcranial elements, and compare its anatomy with that of other known non-sauropodan sauropodomorphs. In general, the cranium of Xingxiulong is more similar to those of more basal sauropodomorphs than to sauropodiforms, as evidenced by features such as an only slightly concave dorsal margin of the postorbital, a caudally placed rostral margin of the infratemporal fenestra not extending below the orbit, and long and slender basipterygoid processes divergent from each other at an angle of approximately 80 degrees. However, its postcranial axial skeleton possesses some unique or relatively derived features among basal sauropodomorphs, such as four sacral vertebrae and caudal dorsal vertebrae with laterally expanded neural spine tables. This provides future workers with a reassessment of non-sauropodan sauropodomorphs through the lens of Xingxiulong chengi, which will serve to increase our knowledge on the anatomy, phylogeny, and furthermore, evolution of sauropodomorph dinosaurs. Anat Rec, 303:772–789, 2020. © 2019 American Association for Anatomy

Key words: Xingxiulong chengi; Sauropodomorpha; Dinosauria; Lufeng formation; lower Jurassic

Additional Supporting Information may be found in the online version of this article.

Grant sponsor: National Natural Science Foundation of China; Grant numbers: 41688103, 41872021, 41472020; Grant sponsor: The Strategic Priority Research Program of Chinese Academy of Sciences; Grant number: XDB26000000.

*Correspondence to: Hai-Lu You, Key Laboratory of Vertebrate Evolution and Human Origins, Institute of Vertebrate Paleontology and Paleoanthropology, Chinese Academy of Sciences, 142 Xizhimenwai Street, Beijing 100044, China. E-mail: youhailu@ivpp.ac.cn

Received 24 September 2018; Revised 5 September 2019; Accepted 13 September 2019.

DOI: 10.1002/ar.24305
Published online 5 December 2019 in Wiley Online Library (wileyonlinelibrary.com).

Sauropodomorpha represents one of the major clades of dinosaurs (Brusatte et al., 2010; Langer, 2014). It is the earliest known group of dinosaurs (Carnian Stage of Late Triassic) and presents a high diversification of at least seven genera in South America (Müller et al., 2018; Pretto et al., 2019). During the Norian Stage of the Late Triassic, it achieved a global distribution and approached large body sizes of 10 tons (Apaldetti et al., 2018). The end-Triassic extinction, although removing many previously dominant groups, gave rise to the true age of dinosaurs with a great radiation of sauropodomorphs (Padian, 2013; McPhee et al., 2017). However, the relationships among Early Jurassic sauropodomorphs are highly debated, and this has direct bearing on the origin of Sauropoda, the clade which includes the largest land animals to ever walk the Earth (McPhee and Choiniere, 2017; Chapelle and Choiniere, 2018; Regalado Fernandez et al., 2018; Zhang et al., 2018).

The Lower Jurassic Lufeng Formation in Yunnan Province of southwestern China preserves one of the best terrestrial vertebrate faunas in the world, and sauropodomorphs are the most abundant in terms of both named taxa and collected specimens. To date, eight genera and 10 species of non-sauropodan sauropodomorphs have been reported from the Lufeng Formation in the Lufeng and Chuanjie basins of the Lufeng area, including Lufengosaurus huenei, "Gyposaurus" sinensis, Yunnanosaurus huangi, Lufengosaurus magnus, Yunnanosaurus robustus, Jingshanosaurus xinwaensis, Chuxiongosaurus lufengensis, Xixiposaurus suni, Xingxiulong chengi, and Yizhousaurus sunae (Young, 1941a, 1941b, 1942, 1947, 1951; Zhang and Yang, 1995; Lü et al., 2010; Sekiya, 2010; Wang et al., 2017; Zhang et al., 2018). However, none of these taxa have been fully described, with only the cranial material of Lufengosaurus and Yunnanosaurus having received detailed redescription (Barrett et al., 2005; Barrett et al., 2007). The lack of detailed morphological studies on these taxa limits their usefulness for further phylogenetic and other studies interested in the early history of sauropodomorph diversification.

Xingxiulong chengi was initially reported by Wang et al. (2017). Represented by three overlapping partial skeletons from one quarry, this species is one of the most completely known non-sauropodan sauropodomorphs globally. Here its axial skeleton is described in detail, in hopes of contributing to further comparative and systematic studies on basal sauropodomorph dinosaurs.

MATERIALS AND METHODS

Materials

The axial skeleton of Xingxiulong is preserved in the holotype (LFGT-D0002) and two paratypes (LFGT-D0001 and LFGT-D0003). LFGT-D0002 includes the partial skull and mandible, atlas–axis complex, three cervical vertebrae (possibly C7–C9), nine dorsal vertebrae (possibly D6–D14; note that they were incorrectly listed as "D8–D14" by Wang et al., 2017), four sacral vertebrae, 35 proximal caudal vertebrae, and fragments of ribs and chevrons (Fig. 1C). LFGT-D0001 preserves a nearly complete cervical series except for the atlas (thus, axial axis and C3–C10), complete dorsal series (D1–D14), four sacral vertebrae, and 19 proximal caudal vertebrae (possibly Ca2–Ca21; Fig. 1B; note LFGT-D0001 was incorrectly labeled as LFGT-D0003 in Supplementary figure S2 of Wang et al., 2017). LFGT-D0003 preserves the partial skull and mandible, eight cervical vertebrae (possibly C3–10), 12 dorsal vertebrae (possibly D1–D12; note that they were incorrectly given as "D1–D14" by Wang et al., 2017), nearly complete sacral vertebral series, and fragments of ribs and chevrons (Fig. 1D).

Methods

The anatomical terminology of this work follows veterinary terms (e.g., cranial, caudal) rather than traditional directional terms (e.g., anterior, posterior). The vertebral laminae nomenclature follows the scheme of Wilson (1999).

Anatomical Abbreviations

af, articular facet; ana, atlantal neural arch; ang, angular; ar, articular; ax, axis; bo, basioccipital; bpt, basipterygoid process; bt, basal tuber; C, cervical vertebra; Ca, caudal vertebra; cau, caudal vertebra; cb, ceratobranchial; ch, chevron; cr, cervical rib; cs, caudosacral; D, dorsal vertebra; d, dentary; db, distal blade; di, diapophysis; dr, dorsal rib; ds, dorsosacral; ecp, ectopterygoid; f, frontal; hc, haemal canal; il, ilium; inc, intercentrum; j, jugal; l, lachrymal; lc, lateral condyle; lsp, laterosphenoid; ma, maxilla; mc, medial condyle; mpp, medial pyramidal process of the articular; n, nasal; ns, neural spine; nst, neural spine table; od, odontoid;

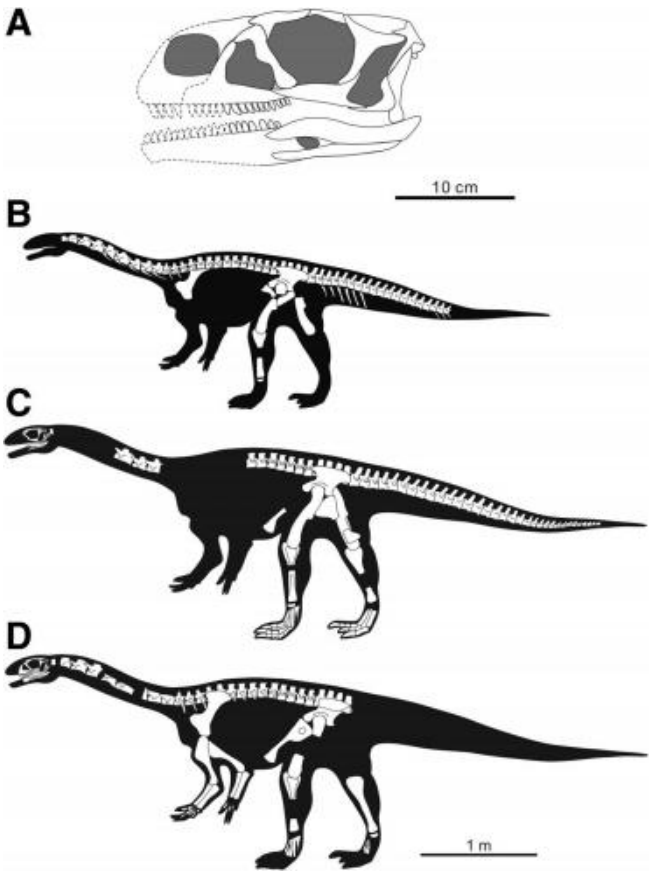

Fig. 1. Reconstruction of the cranium and the three skeletons of Xingxiulong. (A) reconstruction of the cranium based on LFGT-D0002 and LFGT-D0003. (B) Reconstruction of the skeleton of LFGT-D0001. (C) Reconstruction of the skeleton LFGT-D0002, holotype. (D) Reconstruction of the skeleton of LFGT-D0003.

p, parietal; pa, parapophysis; par, paroccipital process; pat, proatlas; pcdl, caudal centrodiapophyseal lamina; po, postorbital; podl, postzygodiapophyseal lamina; popf, postparietal fenestra; poz, postzygapophysis; ppdl, parapodiapophyseal lamina; prdl, prezygodiapophyseal lamina; pre, prearticular; prf, prefrontal; prz, prezygapophysis; ps, parasphenoid; pt, pterygoid; pu, pubis; q, quadrate; qj, quadratojugal; r, rib; s1, first primordial sacral; s2, second primordial sacral; sa, surangular; sk, fragments of skull roof; so, supraoccipital; sq, squamosal; sr, sacral rib; stf, supratemporal fenestra; tmp, tab-like medial process of the retroarticular process; tp, transverse process; vk, ventral keel; vr, ventral ridge; vs, ventral sulcus.

Institutional Abbreviations

LFGT, Bureau of Land and Resources of Lufeng County, Lufeng, Yunnan, China.

RESULTS

Cranium

The holotype (LFGT-D0002) preserves the portion of the skull and articulated mandible caudal to the orbit, but most of the preserved bones are distorted and severely misaligned (Fig. 2). LFGT-D0003 preserves the skull and articulated mandible without the rostral portion, which is adhered to the proximal caudal vertebrae of LFGT-D0002; only the left side of the cranium has been exposed (Fig. 3). Its skull roof was crushed and only represented by some fragments of bones that are difficult to interpret. Most of the left mandible and a fragment of the right mandible are articulated with the skull; however, the left mandible lacks its rostral end, and the lateral surface of its caudal part has been crushed. LFGT-D0003 is better preserved and less crushed than LFGT-D0002, and it forms the main focus of the following description.

In lateral view, the cranial openings are moderately large relative to the skull (Fig. 3). The external naris has not been preserved in either specimen. The antorbital fenestra is subtriangular in outline with a roughly vertical rostral border and bounded by the nasal, lacrimal, and maxilla. The orbit is large and subcircular. The infratemporal fenestra is subrectangular, and its rostral margin is located caudally to the caudal margin of the orbit, similar to the condition in Plateosaurus (AMNH FARB 6810; Prieto-Márquez and Norell, 2011) but contrary to the more rostrally located margin in Lufengosaurus (IVPP V15; Barrett et al., 2005), Yunnanosaurus (NGMJ 004546; Barrett et al., 2007), and Jingshanosaurus (LFGT-ZLJ0113; Zhang and Yang, 1995). The supratemporal fenestra is visible in lateral view and has a subtriangular outline in dorsal view. It should be noted that the right supratemporal fenestra of the holotype is compressed rostrocaudally, and therefore it looks more oval, with its long axis being more transversely oriented (Fig. 2). On the lateral surface of the mandible, an external mandibular fenestra is bounded rostrally by the dentary, dorsally by the surangular, and ventrally by the angular (Fig. 3). However, the exact shape and size of this fenestra is difficult to ascertain.

Maxilla. The maxilla preserves its caudal three quarters, including the caudal part of the ascending process and the horizontally directed caudal ramus (Fig. 3). The ascending process extends roughly vertically, borders the antorbital fenestra rostrally, and is gently excavated to form the craniomedial wall of the antorbital fossa. This fossa is craniocaudally shorter than the orbit, similar to the condition in most basal sauropodomorphs, but contrary to that of Plateosaurus in which the antorbital fossa is longer than the orbit (AMNH FARB 6810; Prieto-Márquez and Norell, 2011). The caudal ramus is a straight and slender process. It is slightly dorsally convex along most of its length, and gradually decreases in height caudally. The caudal end of the maxilla contacts the lacrimal dorsally and the jugal caudally, although the former is slightly separated by crushing, and the caudal termination is obscured by the jugal. The lateral surface of the maxilla lacks the maxillary ridge present in Lufengosaurus (Barrett et al., 2005). Eleven short maxillary teeth are visible, although the tips of their crowns are encrusted by matrix.

Nasal. The nasal is poorly preserved and only retains its caudal end, which contacts the ascending process of the maxilla ventrally and the lacrimal caudally (Fig. 3). However, the displacement of the frontal and prefrontal makes it difficult to confirm the exact articulations among them.

Lacrimal. The rostral ramus of the lacrimal is missing. The shaft of the lacrimal is oriented rostrodorsal-caudoventrally. The dorsal half of the shaft is slightly bowed caudolaterally due to a prominent rostromedially extending flange (Fig. 3). This flange was described as "medial lamina" by Barrett et al. (2005) and is also present in Lufengosaurus (Barrett et al., 2005), Coloradisaurus (Apaldetti et al., 2014), Massospondylus (BP/1/5241; Chapelle and Choiniere, 2018), Adeopapposaurus (PVSJ610; Martínez, 2009), and Plateosaurus (Prieto-Márquez and Norell, 2011), but absent in Yunnanosaurus (Barrett et al., 2007) and Jingshanosaurus (Zhang and Yang, 1995); however, the lamina in Xingxiulong seems to be longitudinally shorter than those in other non-sauropodan sauropodomorphs. The shaft ventral to the lamina is constricted, whereupon it expands again toward its ventral termination.

Prefrontal. The prefrontal is displaced slightly ventrally from its natural position and exposed laterodorsally (Fig. 3). It comprises the rostrodorsal margin of the orbit. Caudally, the prefrontal articulates with the rostral end of the frontal. Due to the poor preservation, more anatomical details of the prefrontal cannot be determined.

Frontal. The frontal is better preserved in the holotype than in LFGT-D0003 (Figs. 2 and 3). The two frontals are fused to each other. They are transversely broad elements roofing the skull medial to the orbital, with a large contribution to the dorsal margin of the orbital. The dorsal surface of the frontal is flat rostrally and becomes slightly concave caudally. A lateroventral process forms a short contact with the postorbital ventrally. Caudally, the frontal contacts the parietal, and the caudoventral portion of the frontal forms a part of the rostral margin of the supratemporal fenestra.

Parietal. The paired parietals are well preserved in the holotype (Fig. 2). They are fused rostrally, separated caudally, and form the dorsal margin of the postparietal fenestra. A stout rostrolateral process arises from the main body of the parietal rostrolaterally, contacts the

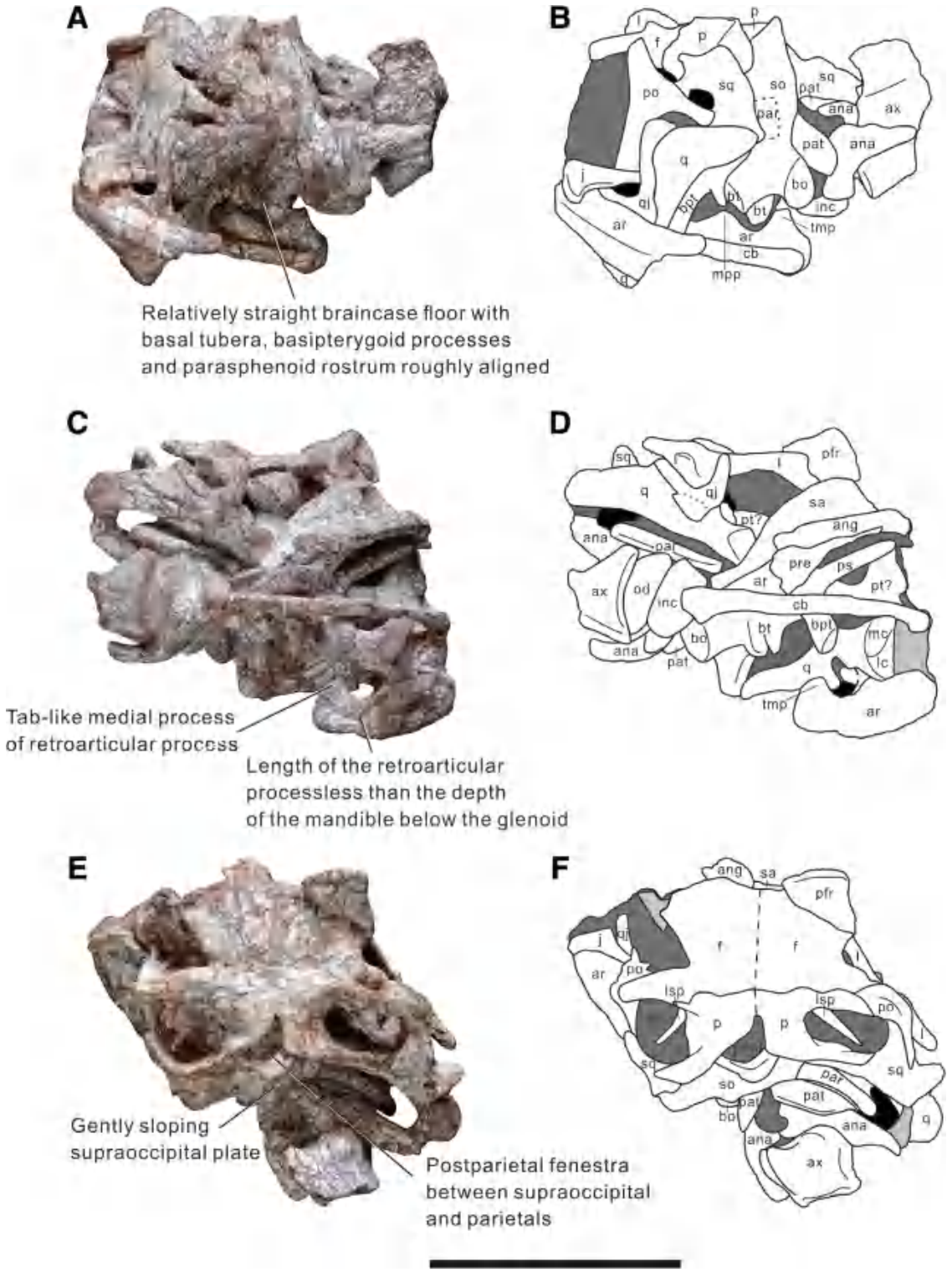

Fig. 2. Skull, mandible, and atlas-axis (LFGT-D0002, holotype) in (A, B) left lateral, ventral (C, D), and dorsal (E, F) views. Scale bar = 10 cm.

frontal, and forms the rostromedial margin of the supratemporal fenestra. Laterally, it contacts the dorsal process of the postorbital. The main body of the parietal contributes to the supratemporal fossa that is deeply excavated laterally, as in Plateosaurus (AMNH FARB 6810; Prieto-Márquez and Norell, 2011), Lufengosaurus (Barrett et al., 2005), and Yizhousaurus (Zhang et al., 2018), and this fossa is located right on the frontal–parietal suture. The

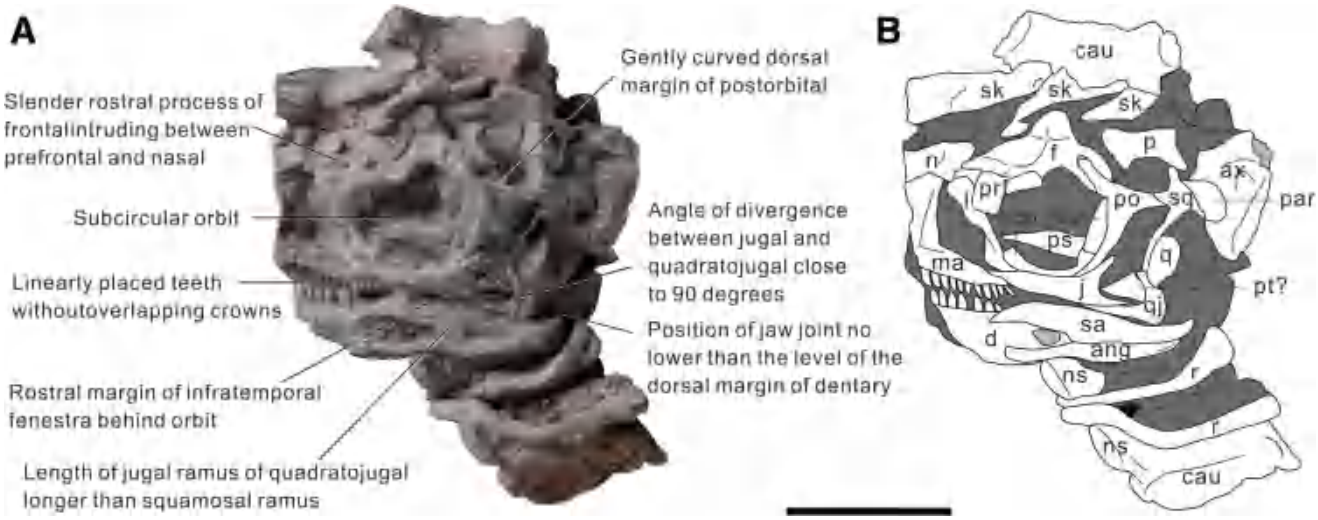

Fig. 3. Skull, mandible, and axis (LFGT-D0003) in left lateral views. Scale bar = 10 cm.

caudolateral process forms the caudal margin of the supratemporal fenestra. In occipital view, this process is triangular.

Postorbital. The postorbital is a triradiate bone with a long ventral process and two short processes that are directed rostrodorsally and caudodorsally, respectively (Fig. 3). The dorsal margin of the postorbital is only slightly concave. The ventral process is caudally bowed. It tapers ventrally and contacts the rostral surface of the dorsal process of the jugal for a moderate length, similar to the condition in Lufengosaurus; in contrast, the postorbital of Yunnanosaurus has a simple tongue-and-groove contact with the jugal (Barrett et al., 2007). The rostrodorsal process is slender; it inserts into the two rami of the caudal process of the frontal. The caudodorsal process is slightly shorter than the rostrodorsal one and projects more medially. In lateral view, the ventral and rostrodorsal processes form most of the caudal and caudodorsal orbital rims, whereas the ventral and caudodorsal processes define the rostrodorsal margin of the infratemporal fenestra; the caudodorsal process also forms the lateral margin of the supratemporal fenestra.

Jugal. The jugal is a triradiate bone and consists of a rostral process, a caudodorsal one, and a caudal one (Fig. 3). The boss that is present on the central portion at the junction of the three processes in Lufengosaurus is absent in Xingxiulong (Barrett et al., 2005). The rostral process is the most robust and longest, nearly twice as long as the caudal one. It tapers rostrally and contacts the maxilla. The caudodorsal process is slender and short, wrapping the ventral one-third of the postorbital caudally. It projects caudodorsally and diverges from the caudal process at an angle of approximately 80 degrees, resembling although slightly smaller than those in Plateosaurus (AMNH FARB 6810, 80 degrees or 95 degrees; Prieto-Márquez and Norell, 2011), but presenting a larger angle than that seen in Massospondylus (BP/1/5241, 40 degrees; Chapelle and Choiniere, 2018), Lufengosaurus (50 degrees; Barrett et al., 2005), Jingshanosaurus (50 degrees; Zhang and Yang, 1995), Mussaurus (MPM-PV 1813/4, 50 degrees; Pol and Powell, 2007a), Yunnanosaurus (60 degrees; Barrett et al., 2007) and Xixiposaurus (60 degrees; Sekiya, 2010). The caudal process is longer and slenderer than the caudodorsal one.

Squamosal. The squamosal consists of a robust main body and four rami: the rostral, ventral, caudal, and medial ones (Fig. 3). Its general outline resembles that of most basal sauropodomorphs. The rostral ramus is short and robust, and articulates with the postorbital rostrally. The medial ramus is widened at its base, but its medial end is obscured by the parietal in dorsal view. The V-shaped slender ventral ramus is the longest among all the rami, and tapers ventrally to a small contact with the quadratojugal. The caudal ramus is the slenderest one and contacts the paroccipital process medially.

Quadratojugal. The quadratojugal is a slender element that gives rise to a rostral ramus and a dorsal one (Fig. 3). In lateral view, the two rami diverge from each other at an angle close to 90 degrees, contrary to those in Lufengosaurus (45 degrees; Barrett et al., 2005), Yunnanosaurus (60 degrees; Barrett et al., 2007), and Jingshanosaurus (110 degrees; Zhang and Yang, 1995), and define the caudoventral margin of the infratemporal fenestra. The rostral ramus is longer and slenderer than the dorsal one, tapering rostrally past the rostral margin of the infratemporal fenestra, resembling that in Lufengosaurus (Barrett et al., 2005). The dorsal ramus is slightly expanded at its dorsal end and articulates with the quadrate caudally. Caudally, the margin of the main body is rounded, lacking the caudoventral process present in most non-sauropodan sauropodomorphs (e.g., Lufengosaurus, Yunnanosaurus, Jingshanosaurus, and Plateosaurus).

Quadrate. Both quadrates are better preserved in the holotype than in LFGT-D0003 (Fig. 2). The dorsal end of the quadrate constitutes the head that articulates with the ventral surface of the squamosal. The right quadrate head is exposed dorsally and mediolaterally compressed.

Ventral to the quadrate head, the main shaft gives rise to two laminae: the lateral lamina and the medial lamina. The lateral lamina has a reversed D-shaped profile and extends nearly half of the total length of the shaft. Its dorsal part meets the ventral ramus of the squamosal and the ventral part contacts the dorsal ramus of the quadratojugal rostrally. The exposed dorsal end of the medial lamina diverges at an angle of approximately 90 degrees from the lateral lamina. The middle part of the medial lamina is covered by matrix, whereas the ventral part can be discerned caudolaterally; it is much wider rostrocaudally and longer dorsoventrally than the lateral lamina, extending three-quarters of the shaft, and contacts the putative pterygoid. In lateral view, the shaft of the quadrate is slightly twisted. Its caudolateral surface is shallowly excavated while the rostromedial surface is more concave. Distally, the shaft of the quadrate is expanded both transversely and rostrocaudally, forming the distal articulation with the mandible. On the distal articular surface of the quadrate, the lateral condyle is larger and more dorsally located than the medial condyle, contrasting with that of Plateosaurus in which the lateral condyle is more ventrally situated than the medial one (Prieto-Márquez and Norell, 2011). The ventral surface of the lateral condyle is concave, whereas that of the medial condyle is relatively flat. The presence of a quadrate foramen cannot be determined.

Supraoccipital. The dorsocaudal surface of the supraoccipital is inclined slightly rostrally. It is slightly dorsoventrally higher than transversely wide. Dorsally, it contacts the parietals and forms the caudal margin of the postparietal fenestra (Fig. 2). This postparietal fenestra has a subtriangular profile and opens dorsally; however, its size is probably enlarged due to the torsion of the supraoccipital. In caudal view, the supraoccipital sutures with the parietals dorsolaterally and the exoccipital-opisthotic ventrolaterally. On the caudal surface of the supraoccipital, a low and rounded ridge extends along the midline of this bone from the dorsal tip to the dorsal margin of the foramen magnum, which is a common feature seen in other non-sauropodan sauropodomorphs (e.g., Lufengosaurus; Plateosaurus, AMNH FARB 6810; Coloradisaurus, PVL 3967). Lateral to this ridge, the caudal surface is concave. The ventral margin of the supraoccipital is slightly concave and contributes to the dorsal border of the foramen magnum.

Paroccipital process. The boundary between the exoccipital and opisthotic cannot be discerned and the two bones are fused into a single element that comprises the paroccipital process. Only the mediorostral end of the left process is preserved, whereas the right one is completely preserved, although it is covered by the right quadrate laterally (Fig. 2). The exoccipital part of the paroccipital process forms the lateral border of the foramen magnum and contacts the occipital condyle ventrally. The paroccipital process projects ventrolaterally from the suture with the supraoccipital. It is dorsoventrally high at its base but becomes constricted at the central region. Viewed dorsally, it is slightly curved, and its caudal surface contacts the proatlas. Close to its base, the paroccipital process contacts the squamosal medially. The distal end of the paroccipital process is missing in LFGT-D0003; however, in the holotype the distal end of the left paroccipital process appears expanded.

Basioccipital. The basioccipital forms the ventral margin of the foramen magnum and contacts the exoccipital. The caudal end of the basioccipital is partially covered by the cervical elements (Fig. 2). Based on its exposed left half, the occipital condyle is convex caudally, and has a subcrescentic profile. The rostroventral part of the basioccipital contributes to the basal tubera. In ventral view, the neck between the occipital condyle and the basal tubera is slightly constricted and depressed. The basal tubera are subcircular processes that are ventrolaterally directed. The basioccipital component of the basal tubera is slightly larger than the basisphenoid component, and the ventral part of the former is located caudally to the latter; however, the dorsal part becomes more medially placed relative to the basisphenoid component. A ridge is developed transversely along the notch separated between the basal tuberae. In lateral view, the ventral border of the occipital condyle is situated dorsal to the level of the basal tubera and parasphenoid rostrum, as in Adeopapposaurus (PVSJ610; Martínez, 2009).

Basisphenoid. The basisphenoid is only partially visible in ventral view (Fig. 2). The caudoventral part of the basisphenoid (the basisphenoid component of the basal tubera) contacts the opisthotic dorsolaterally. A circular median fossa is developed on the ventral surface of the rostral part and located between the basal tubera and the basipterygoid processes. The rostroventral portion of the basisphenoid is composed primarily of the paired basipterygoid processes. The basipterygoid processes are long, slender and ventrolaterally projected, contrasting with the short, robust ones in Lufengosaurus (Barrett et al., 2005) and Jingshanosaurus (Zhang and Yang, 1995). The basipterygoid process has a subcircular cross section and is slightly expanded at its distal end.

Parasphenoid. The parasphenoid rostrum arises rostrally from the base of the basipterygoid processes (Fig. 2). Its pointed rostral end appears complete. It is transversely compressed, elongate, and higher than wide. In lateral view, the parasphenoid rostrum and the base of the basipterygoid processes are roughly aligned with the occipital condyle and the basal tuberae. The subsellar recess located at the base of the parasphenoid rostrum that was discussed by Bronzati and Rauhut (2018) is shallow in Xingxiulong.

Dentary. The rostral end of the dentary is missing, and the caudal end has been crushed between the surangular and the angular (Fig. 3). It is dorsoventrally high, and reaches its greatest height close to its contact with the post-dentary bones. Six teeth and an inferred seventh tooth are present in the dentary. There is no evidence to suggest that a lateral ridge is present on the lateral surface of the dentary.

Surangular. The surangular is somewhat crushed dorsoventrally (Fig. 3). Viewed laterally, it is a long element and extends rostrally far beyond the external mandibular fenestra, forming the dorsal and caudal border of this fenestra. The rostral portion dorsal to the external mandibular fenestra is convex dorsally and concave

ventrally. Immediately caudal to the fenestra, the surangular reaches its deepest greatest depth and gradually decreases in depth caudally. In the holotype, the caudal portion of the right surangular is preserved (Fig. 2), and its dorsal margin is strongly convex. A large foramen is present on the lateral surface of the preserved rostral end, and this probably corresponds to the position of the external mandibular fenestra. Ventrally, the surangular has a long contact with the angular. Its caudal end articulates with the angular ventrolaterally and the prearticular ventromedially.

Angular. The angular is slightly shorter and slenderer than the surangular (Fig. 3). It borders the external mandibular fenestra ventrally and ends rostrally to it. The rostral extension of both the surangular and the angular beyond the external mandibular fenestra contrasts with the short extension of those elements in Lufengosaurus, Yunnanosaurus, and Jingshanosaurus, and more resembles the condition in Plateosaurus (AMNH FARB 6810; Prieto-Márquez and Norell, 2011) and Adeopapposaurus (PVSJ610; Martínez, 2009). The preserved caudal portion of the angular in the holotype possesses a dorsal eminence close to its caudal end (Fig. 2). It contacts the surangular dorsally and the prearticular medially.

Prearticular. In the holotype, the right prearticular is preserved in ventral and medial views (Fig. 2). It is rostrocaudally elongate and irregularly shaped. The rostral portion is a transversely compressed lamina that articulates with the surangular laterally and the angular ventrolaterally. The caudal portion increases its size and forms a subtriangular plate. It is ventrally convex, but its surface is laterally overlapped by the surangular. The expanded plate of the prearticular contacts the angular laterally and the articular caudally.

Articular. Both articulars are preserved in the holotype. The right one is preserved in articulation with other elements of the mandible, and the left one is isolated (Fig. 2). The articular has an irregular profile. It contacts the prearticular rostrally and the quadrate dorsally. Rostrally, the articular expands medially to form the glenoid fossa, which is bordered medially by a large pyramidal process. An embayment is present behind the glenoid along the medial edge. The caudal end is expanded to form a sub-rounded dorsally facing surface. It should be noted that a dorsally projected, laminar, and tab-like process is developed on the medial surface of the retroarticular process (Fig. 2). This tab-like medial process in Xingxiulong appears larger, more distinct and more caudally located than that of Coloradisaurus (PVL 3967; Apaldetti et al., 2014). Some other non-sauropodan sauropodomorphs from Lufeng, such as Jingshanosaurus (Zhang and Yang, 1995) and Yizhousaurus (Zhang et al., 2018) also possess this tab-like medial process.

Ceratobranchial. A ceratobranchial is preserved in the holotype (Fig. 2). It is elongate, thin, and slightly sinuous, with a total length of 98 mm. This element is mediolaterally compressed and dorsoventrally deeper than transversely wide. Both ends are expanded but more so in the rostral end than in the caudal.

Dentition. The teeth of Xingxiulong are poorly preserved, with all the premaxillary teeth, and the mesial maxillary and dentary teeth missing. Furthermore, the mesial and distal margins of the preserved teeth are obscured by close apposition and matrix, and the presence of denticles could not be determined (Fig. 3). The teeth are probably longer than observed because the tips of the crowns are either overlapped by each other or encrusted by matrix. In general, the dentary teeth exhibit a similar morphology to the maxillary teeth, although the dentary teeth are slightly widened mesiodistally. The tooth crowns are almost vertical, symmetrical in labial view, and display little recurvature caudally. The labial surfaces of the crowns are convex and smooth and exhibit no grooves or ridges, or enamel wrinkling.

Postcranial Axial Skeleton

LFGT-D0001 preserves an almost completely articulated axial column, from the axis to the last sacral (see Fig. S1A), as well as the proximal caudals (possibly Ca3–Ca21). The following description of the cervicals and dorsals is mainly based on this specimen (Figs. 4, 5 and 8–11), supplemented with anatomy from the holotype LFGT-D0002 (Figs. 2 and 12) and LFGT-D0003 (Fig. 13). The description of the sacral and caudal vertebrae will focus on the holotype and LFGT-D0001 (Figs. 14–16). All the preserved cervical, dorsal, and caudal vertebrae have their neural arches fully fused to the centra, suggesting all the three individuals were at least subadults.

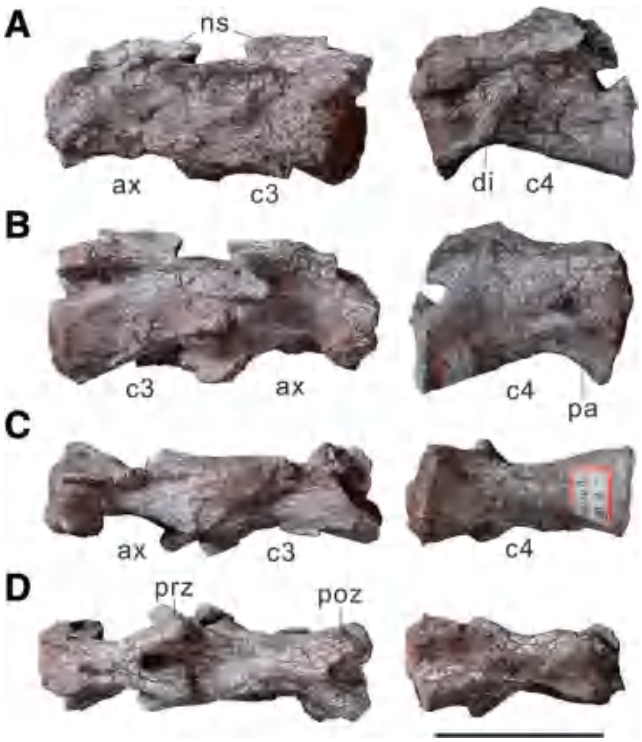

Fig. 4. Axis, the third and fourth cervical vertebrae (LFGT-D0001) in (A) left lateral, (B) right lateral, (C) ventral, and (D) dorsal views. Scale bar = 10 cm.

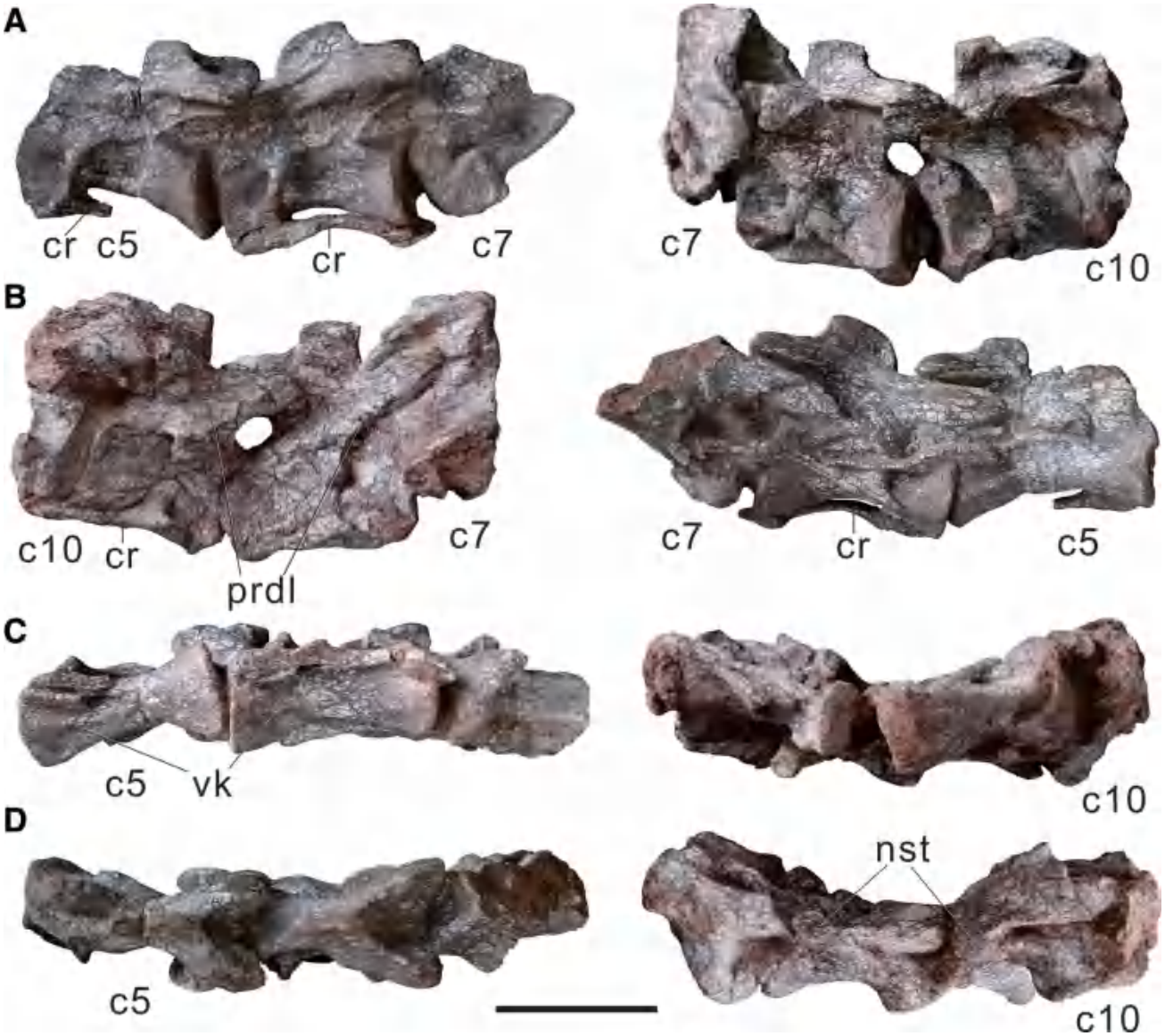

Fig. 5. Fifth to tenth cervical vertebrae (LFGT-D0001) in (A) left lateral, (B) right lateral, (C) ventral, and (D) dorsal views. Scale bar = 10 cm.

Xingxiulong possesses 10 cervical vertebrae, typical for non-eusauropod sauropodomorphs. All cervical centra appear to be amphicoelous (although it is difficult to confirm given that some elements are firmly articulated with each other) and solid inside without the evidence of camerae or camellae.

Proatlas and atlas. In the holotype, both proatlases are preserved almost in articulation with other bones (Fig. 2). They are somewhat crushed and partially obscured by the occipital bones. In dorsal view, the two proatlases diverge caudolaterally from each other, but the angle between them cannot be discerned (Fig. 2). Cranially, they articulate with the dorsolateral margin of the foramen magnum. The lateral surface of the proatlas is convex and its dorsal margin is nearly straight. The medial side borders the neural canal laterally. The caudal end decreases its dorsoventral depth caudally and contacts the atlantal neurapophyses.

The atlas is composed of an intercentrum, an odontoid (pleurocentrum), and two neurapophyses. All the elements are articulated but not fused with each other, although they have been somewhat displaced (Fig. 2). The odontoid is only exposed in ventral view. It is a small, oval element with flat ventral surface. It articulates tightly with the intercentrum cranially and the axis caudally. The intercentrum is visible in ventral and lateral views (Fig. 2). It has a caudal concavity on the ventral surface. In lateral view, the ventral edge is rostrocaudally longer than the dorsal one, forming a subtrapezoid lateral surface. The intercentrum articulates with the occipital condyle cranially and the neurapophyses dorsally. The left neurapophysis is complete cranially but lacks its caudal end. The right one is distorted whereas its elongated

Fig. 6. Seventh cervical vertebra (LFGT-D0002, holotype) in (A) left and (B) right lateral views. Eighth to ninth cervical vertebrae (LFGT-D0002, holotype) in (C) left and (D) right lateral views. Scale bar = 10 cm.

caudal region is more complete than the left (Fig. 2). The cranial end (prezygapophysis) articulates with the proatlas cranially. Viewed dorsally, two medial processes are projected from the left and right neurapophyses, respectively, and surround the neural canal dorsally. The dorsal and lateral surfaces of the main body of the neurapophyses are convex. The caudal end (postzygapophysis) is elongate and slightly curved, with the epipophysis developed on its lateral surface.

Axis. The axial intercentrum is not preserved. The craniocaudal length of the centrum of the axis is 3.19 times the dorsoventral height of its cranial articular surface (Fig. 4), which is slightly greater than that of Lufengosaurus (Young, 1941a), Jingshanosaurus (Zhang and Yang, 1995), and Sarahsaurus (TMM 43646–2; Marsh and Rowe, 2018). Due to the poor preservation of the ventral surface, the presence of a ventral keel cannot be confirmed. The cranial surface of the centrum is slightly broken and appears concave. The lateral and ventral surfaces are moderately compressed. The caudal surface, however, is firmly articulated with the third cervical, so its condition remains unclear. Laterally, the parapophyses occupy the cranioventral corners of the centrum, and are developed as enlarged protuberances. The diapophysis is not developed. The neural arch is strongly fused to the centrum. With their cranial ends broken, the preserved region of the prezygapophyses partly roofs the circular neural canal. The caudal ends of the postzygapophyses are located cranially to the caudal margin of the centrum. The articular facets of the postzygapophyses face almost ventrally. The neural spine is markedly low and merges uniformly with the postzygapophyses. However, the axis in the holotype (Fig. 4), which has a better preserved cranial portion, displays a neural spine that is moderately high with a spur-like projection on its cranial end.

Third to fourth cervical vertebrae. The third cervical vertebra is articulated with the axis, and the fourth cervical is isolated (Fig. 4). In LFGT-D0003, the third cervical only preserves its caudal half and is articulated with the complete but poorly preserved fourth cervical (Fig. 7).

The length of the third cervical centrum is 1.18 times that of the axis, differing from the more elongated cervical 3 of Lufengosaurus (Young, 1941a), Yunnanosaurus (Young, 1942), and Jingshanosaurus (Zhang and Yang, 1995), in which this metric is 1.47, 1.32, and 1.43, respectively. The length of the fourth centrum is 1.35 times that of the axis. The ventral surface of cervical 3 is somewhat damaged and obscured by the rib fragments, so it cannot be confirmed whether a ventral keel is present or not. The ventral keel of cervical 4 is discernible at the cranial end, and diminishes caudally along most of the ventral surface. Both centra of cervicals 3 and 4 are ventrally and laterally compressed, and bear concave lateral surfaces. The lengths of the centra are approximately 2.78 and 2.8 times the height of their cranial surfaces in cervicals 3 and 4, respectively. The parapophyses are more developed and located higher than the parapophyses of the axis. The diapophysis is developed as a small bump in cervical 3. In cervical 4, however, the diapophysis is much more developed, forming a laterally directed, long process.

The neural arches are fused to the centra. No lamination can be seen in either cervical (Fig. 4). The zygapophyses of the two cervicals extend almost parallel to the

Fig. 7. Third to tenth cervical vertebrae (LFGT-D0003) in left lateral view. Scale bar = 10 cm.

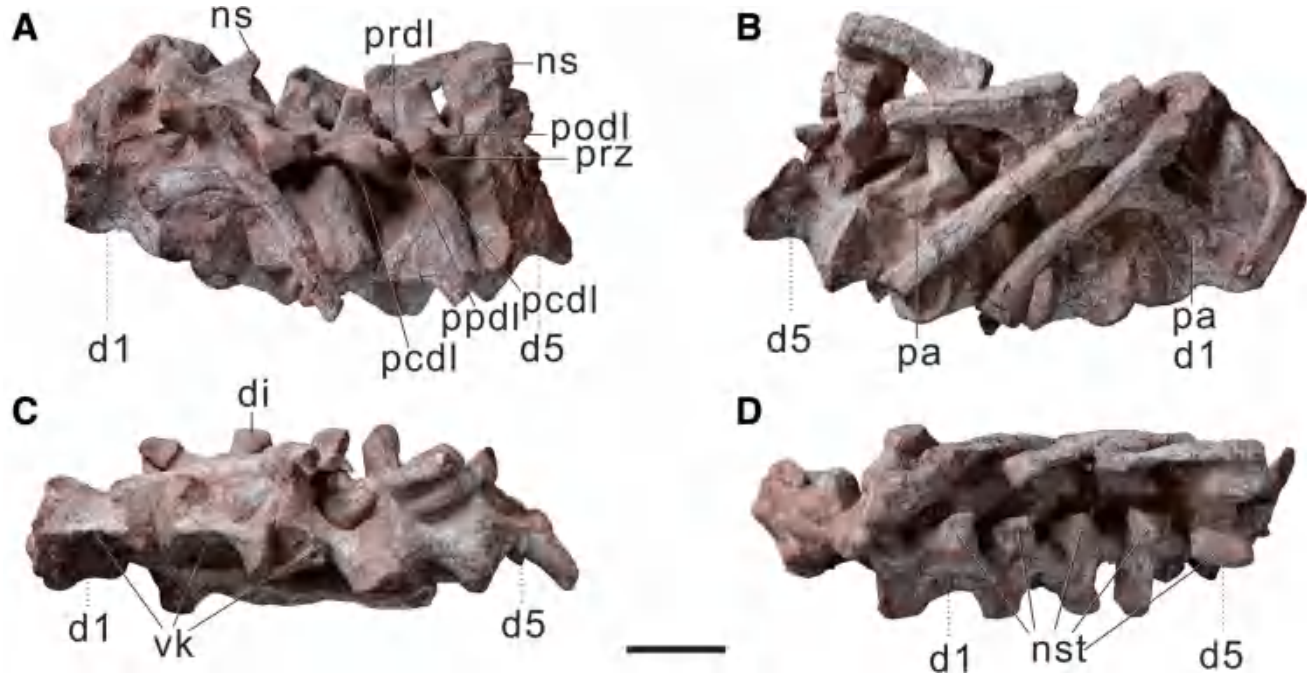

Fig. 8. First to fifth dorsal vertebrae (LFGT-D0001) in (A) left lateral, (B) right lateral, (C) ventral, and (D) dorsal views. Scale bar = 10 cm.

craniocaudal axis of the centra. The prezygapophyses of cervical 3 project much further than the cranial surface of the centrum and have dorsomedially facing articular surfaces. The postzygapophyses extend almost as far caudally as the caudal margin of the centrum. The epipophysis is only slightly developed on the postzygapophyses. Viewed laterally, the neural spine of cervical 3 is low, craniocaudally short, and is of similar dorsoventral height as that of the axis. The neural spine of cervical 4 is broken and displays few anatomical details.

Fifth to seventh cervical vertebrae. LFGT-D0001 preserves nearly complete cervicals 5 and 6 that are articulated with the broken cervical 7 (Fig. 5). In the holotype, cervical 7 is relatively well preserved, although lacking some anatomical details (Fig. 6). Cervicals 5–7 in LFGT-D0003 are very poorly preserved (Fig. 7).

Beginning with the fifth, the cervical centra become elongate in measurement (see Supporting Information), but the length/height ratios of the centra are 2.45 in cervical 5 and 2.15 in cervical 6 (Fig. 5). Compared with the preceding vertebrae, the lateral surfaces of the centra of these cervicals are more concave. The ventral surfaces of the vertebral centra are occupied by a slightly developed ventral keel, which is only present along the cranial half of the centra. The parapophyses are more ventrally positioned than in previous cervicals and become more prominent. The diapophysis is located above the parapophysis, forming an elongated and ventrolaterally directed process that progressively increases its craniocaudal width and mediolateral length from cervicals 5 to 7. The neural arches are slightly higher than those of the cranial cervicals; in cervicals 5 and 6, the height of the neural arch is 0.53 and 0.63 times that of the height of the respective centrum, whereas this ratio is 0.46 and 0.56 in cervicals 3 and 4, respectively. The prezygapophyses are slightly upturned and have dorsomedially facing articular facets. The articular facets of postzygapophyses face ventrolaterally. The prezygodiapophyseal lamina is slightly developed in cervical 7 and is absent in the preceding cervicals. In lateral view, the epipophysis is well developed as a low ridge, and is connected the dorsal surface of the postzygapophysis along its entire length, extending from the neural spine but not beyond the caudal margin of the postzygapophysis. The relatively completely preserved neural spine, which belongs to cervical 6, becomes shorter and higher than in previous cervicals, and lacks a cranial spur-like projection.

Eighth to tenth cervical vertebrae. Cervicals 8 and 9 are well preserved, with the latter articulated with the cranial fragment of the tenth cervical in LFGT-D0001 (Fig. 5). The holotype preserves articulated cervicals 8 and 9, although these are somewhat distorted (Fig. 6), and LFGT-D0003 possesses cervicals 8–10 in poor conditions (Fig. 7).

Compared to the cranial and middle cervical series, cervicals 8–10 are shorter and higher (Fig. 5). The centra retain the same concave lateral surfaces but become wider transversely. In ventral view, the ventral keel is more developed and extends along the entire length of the centra. The condition whereby the ventral keel is less developed in the cranial cervicals and becomes more prominent in the caudal cervicals is similar to that of Lufengosaurus and Yunnanosaurus but differs from that of Yizhousaurus in which the keel is prominent from the cranial cervicals. In cervical 8, a low and short crest is connected between the parapophysis and the caudal end

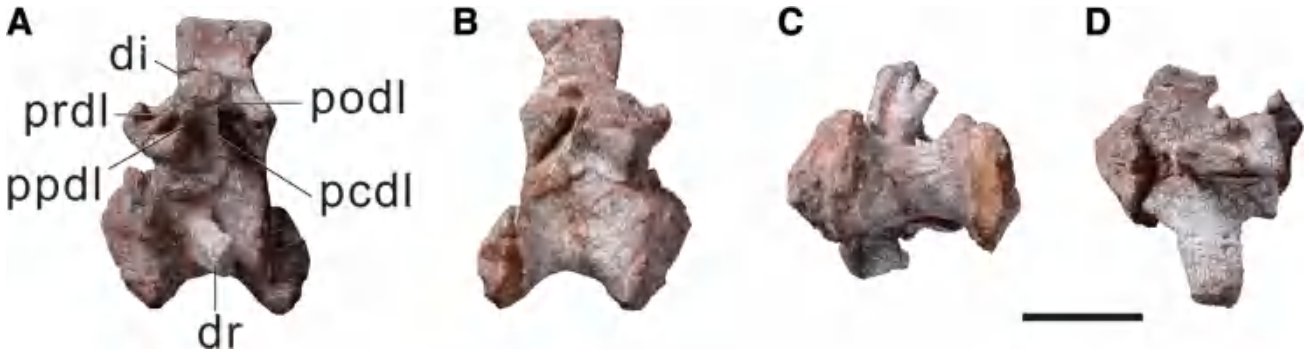

Fig. 9. Sixth dorsal vertebra (LFGT-D0001) in (A) left lateral, (B) right lateral, (C) ventral, and (D) dorsal views. Scale bar = 10 cm.

of the centrum; this crest is absent in cervical 9. The diapophysis is located almost entirely on the neural arch, contrasting with the diapophysis of the preceding cervicals, which is located on the centrum or the suture between the centrum and the neural arch, and becomes much more craniocaudally widened than in the middle of the series. The prezygapophyses are more upturned and have more dorsomedially facing articular facets. As in cervical 7, the prezygodiapophyseal lamina is present in both cervicals, although not as developed as in derived sauropodiforms. The epipophysis is only slightly developed in cervical 8, and disappears in cervical 9. The dorsal end of the neural spine of cervicals 8–10 is laterally expanded, forming a neural spine table, which resembles that of most basal sauropodomorphs.

Dorsal vertebrae. Fourteen dorsal vertebrae are preserved in LFGT-D0001 (Figs. 8–11), nine in the holotype LFGT-D0002 (possibly D6–D14; Fig. 12), and 12 in LFGT-D0003 (D8–D12 in Fig. 13; note that seven cranial dorsals are articulated with the scapula, see fig. 2 in Wang et al., 2017). The elements in LFGT-D0001 are slightly smaller in size than the corresponding ones in the holotype and LFGT-D0003. The isolated dorsal vertebrae in the holotype are slightly amphicoelous, as in other non-eusauropod sauropodomorphs.

First to fourth dorsal vertebrae. The first dorsal vertebra is recognized by the shortened centrum with the presence of a ventral keel and the higher position of the parapophysis than that of the last cervical. The first to fourth dorsal vertebrae are well preserved and tightly articulated with each other and with the fifth dorsal (Fig. 8). The dorsal centra are markedly shorter than the cervical ones and constricted ventrally. Their lateral surfaces are concave, lacking a distinct depression or pleurocoel. The first dorsal centrum is approximately 1.29 longer than it is high, contrasting with the relatively short first dorsal centrum of Jingshanosaurus (Zhang and Yang, 1995) and Lufengosaurus (Young, 1941a), in which this ratio is 1.03 and 0.95, respectively. A ventral keel is well developed on the ventral surface of the centrum of dorsals 1–3, which is distinguished from those of the cervicals by being sharper. It is absent in dorsal 4 and the following series, as occurs in Lufengosaurus, Jingshanosaurus, and Massospondylus (Cooper, 1981); however, this ventral keel is only present on the first dorsal centrum of Adeopapposaurus (Martínez, 2009), and on the 1st, 2nd, 11th, and 12th dorsals of Sarahsaurus (TMM 43646-2, Marsh and Rowe, 2018). Given that the parapophyses are mostly obscured by the ribs in the first three dorsals, their shape remains unclear. Based on the location of the articulated dorsal ribs, the parapophyses are placed at the midlength of the centrum of dorsals 1–3, similar to that of other Lufeng basal sauropodomorphs. The parapophysis of dorsal 4, however, is located dorsally to the suture between the centrum and the neural arch and has an ovoid shape.

The neural arches of the dorsal vertebrae are dorsoventrally lower than their corresponding centra (Fig. 8). The diapophyses are ventrolaterally oriented in dorsals 1–3, and become dorsolaterally directed from dorsal 4 onward. The prezygapophyses are directed cranially, with their articular facets facing dorsomedially. The postzygapophyses are oriented caudolaterally. The lamination of the dorsal vertebrae

Fig. 10. Seventh to ninth dorsal vertebrae (LFGT-D0001) in (A) left lateral, (B) right lateral, (C) ventral, and (D) dorsal views. Scale bar = 10 cm.

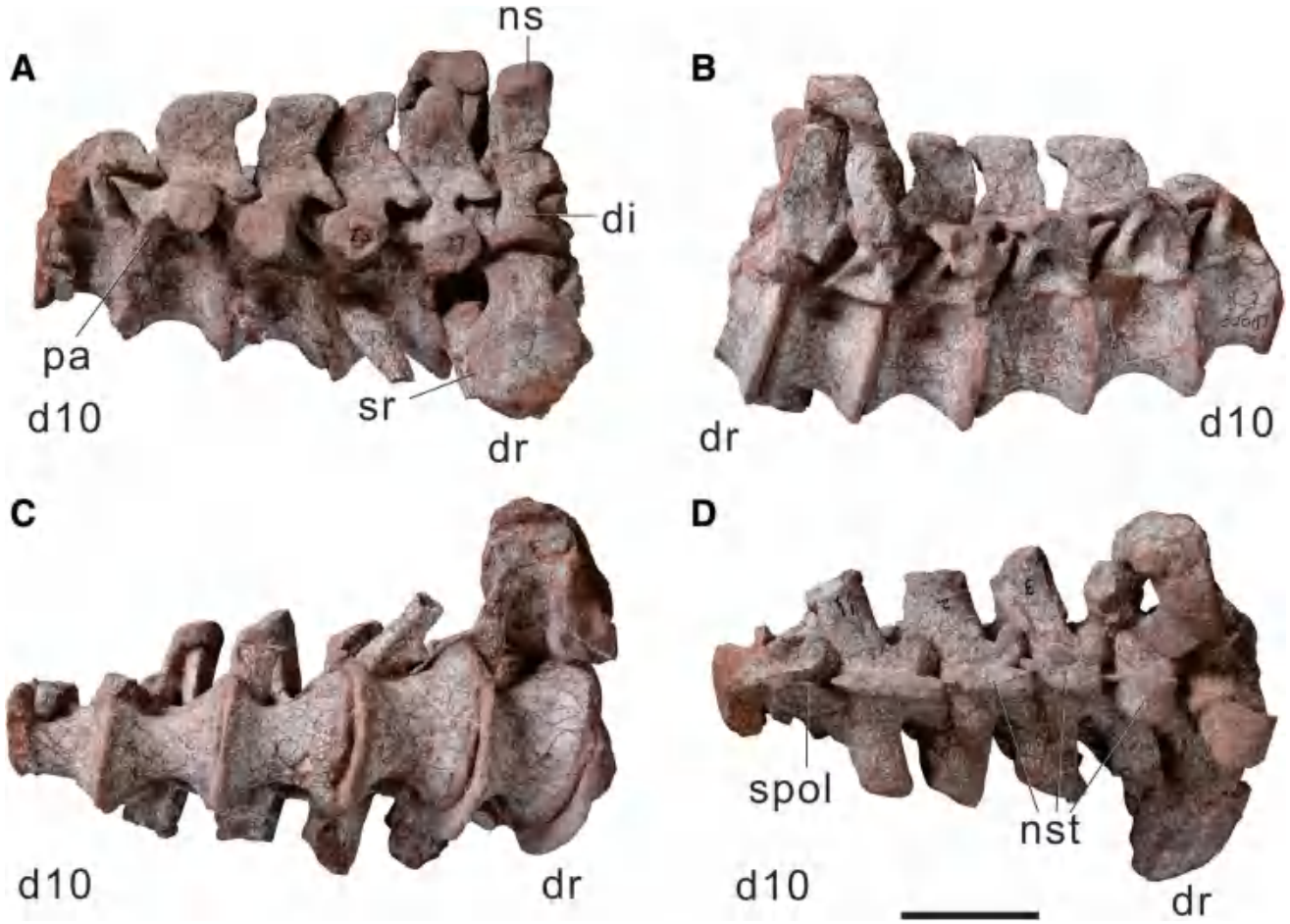

Fig. 11. Tenth to fourteenth dorsal vertebrae and the first sacral vertebra (LFGT-D0001) in (A) left lateral, (B) right lateral, (C) ventral, and (D) dorsal views. Scale bar = 10 cm.

is well developed. Dorsals 1–4 have moderately developed paradiapophyseal, postzygodiapophyseal, and caudal centrodiapophyseal laminae. The prezygodiapophyseal lamina is developed in the third and fourth dorsals; however, whether this lamina is also present in the preceding two elements cannot be ascertained due to the poor preservation.

Fig. 12. Sixth to fourteenth dorsal vertebrae (LFGT-D0002, holotype) in (A) left and (B) right lateral views. Scale bar = 10 cm.

The neural spines of the cranial four dorsals are low and short, with their shapes being subrectangular in lateral view. Dorsally, the neural spine is expanded to plate-like summits (Fig. 8D), with the craniocaudal length of the dorsal surface subequal to its transverse width, as in most non-sauropodan sauropodomorphs such as Jingshanosaurus (Zhang and Yang, 1995), Plateosaurus (MB R 4430 skelett C), and Sarahsaurus (Marsh and Rowe, 2018).

Fifth to ninth dorsal vertebrae. The fifth dorsal vertebra is articulated with the previous dorsal vertebrae (Fig. 8), whereas the sixth dorsal is isolated (Fig. 9). The seventh to ninth dorsals are articulated with one another (Fig. 10). The holotype preserves the sixth to ninth dorsals (Fig. 12), and LFGT-D0003 preserves the fifth and ninth dorsals, among which the eighth and ninth dorsals (Fig. 13) are better preserved than the fifth to the seventh dorsals that are articulated with the scapula (see Fig. 2 in Wang et al., 2017).

In general, the dorsal centra are shorter than in the preceding elements, with their cranial articular faces being higher than they are craniocaudally long. As in dorsal 4, the parapophysis of dorsal 5 is also situated just above the suture between the centrum and the neural

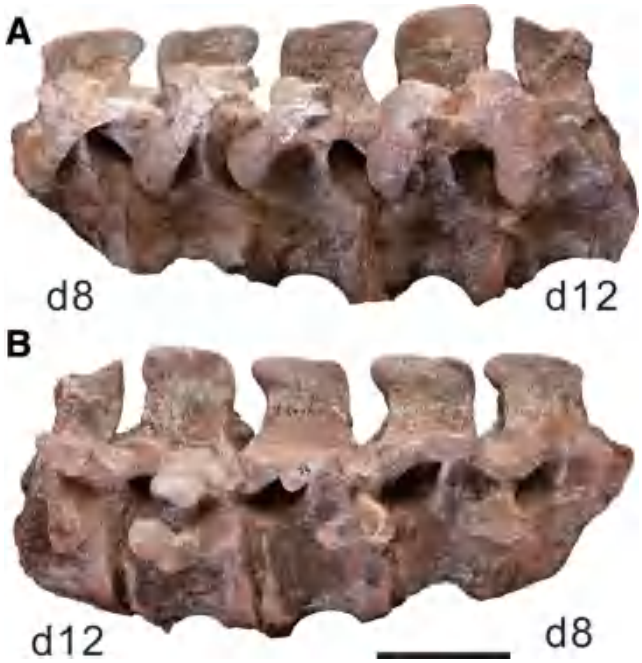

Fig. 13. Eighth to twelfth dorsal vertebrae (LFGT-D0003) in (A) left and (B) right lateral views. Scale bar = 10 cm.

arch (Fig. 7). The condition of dorsal 6 is difficult to assess due to crushing. Beginning with the seventh vertebra, the parapophyses migrate both dorsally and cranially, and are placed entirely on the cranial end of the neural arch (Fig. 10). The diapophyses are more robust and longer than the preceding ones and directed dorsolaterally. The prezygapophyses are relatively short and directed cranially, with dorsally facing facets. The prezygodiapophyseal lamina is developed in dorsals 5–7 but is absent in the caudal dorsals. Paradiapophyseal, postzygadiapophyseal, and caudal centrodiapophyseal laminae are developed in dorsals 6–9. Compared to that of the more cranial dorsals, the neural spine becomes progressively higher, longer and transversely narrower, and a plate-like apex is absent. In LFGT-D0001, the length to height ratio of the neural spines of dorsals 5–9 is 0.80, 0.98, 1.13, 1.16, and 1.27, respectively. A projecting caudodorsal corner of the neural spine is present in dorsals 6–9, forming a concave caudal margin, as opposed to the relatively straight margins seen in Lufengosaurus (Young, 1941a), Yunnanosaurus (Young, 1942), and Jingshanosaurus (Zhang and Yang, 1995).

Tenth to fourteenth dorsal vertebrae. The 10th to 14th dorsal vertebrae are nearly completely preserved in LFGT-D0001 (Fig. 11) and the holotype (Fig. 12). LFGT-D0003 preserves the 10th to 12th dorsals in articulation (Fig. 13).

The centra are longer and higher than in the preceding dorsal vertebrae. The neural arches become taller (Fig. 11). The diapophyses increase their lengths and robustness and are almost horizontally oriented. The pre- and postzygapophyses of most dorsals extend beyond the cranial and caudal articular margins of the centra, respectively, except for dorsals 13 and 14, in which the postzygapophyses do not extend as far as the caudal margins of their

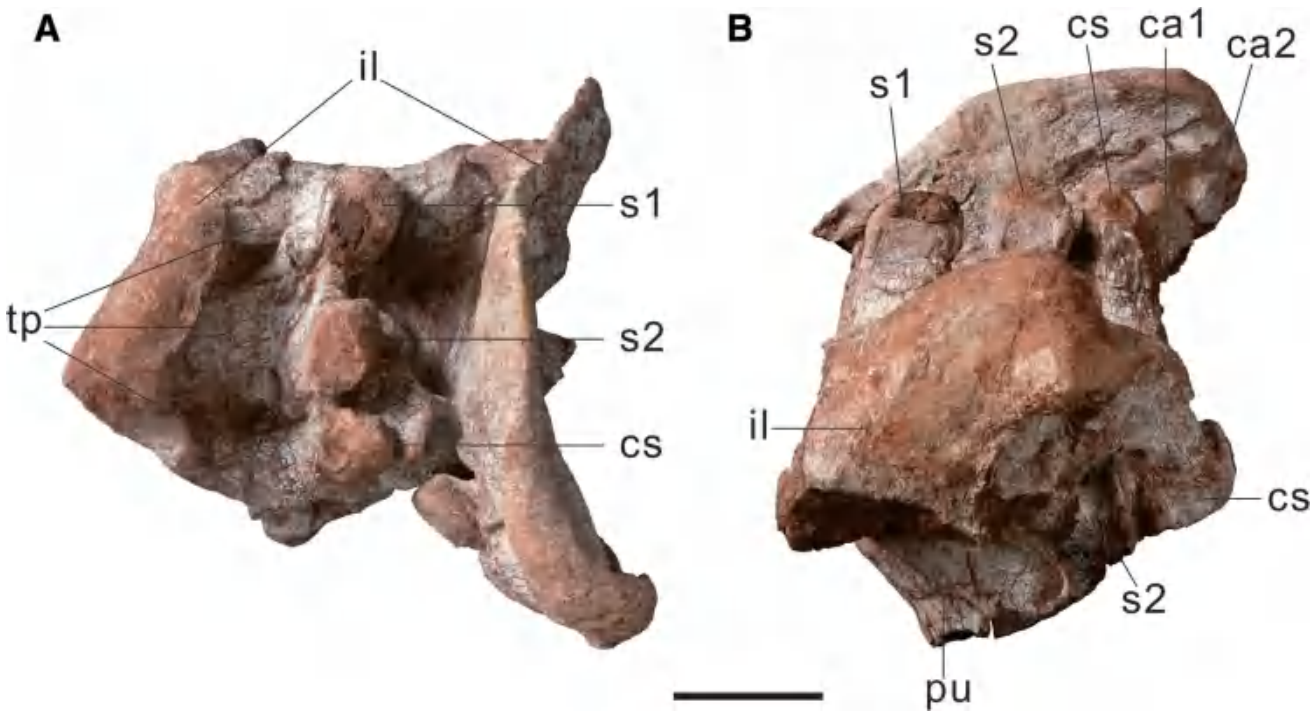

Fig. 14. Second to fourth sacral vertebrae articulated with the ilium (LFGT-D0001) in (A) dorsal and (B) left lateral views. Scale bar = 10 cm.

Fig. 15. (A, B) Caudal vertebrae 1–35 (LFGT-D0002, holotype) in left lateral view. C, Caudal vertebrae 1–8 (LFGT-D0002, holotype) in ventral view. Scale bar = 10 cm.

corresponding centra. As in the middle series, dorsals 10–14 also display paradiapophyseal, postzygadiapophyseal, and caudal centrodiapophyseal laminae; however, the paradiapophyseal lamina is remarkably reduced in the caudal dorsals. The neural spines of dorsals 10–13 are similar in general with those of preceding dorsals; the ratio of length to height of dorsals 11–13 is 1.22, 0.87, and 0.96, respectively. However, the neural spine of dorsal 14 increases its height and length, with a length to height ratio of 0.81, and lacks a projecting caudodorsal corner that is present in preceding dorsals. Furthermore, at least the last three dorsals display a neural spine with a laterally expanded dorsal table, although not as prominent as that of the cranial dorsals (Fig. 11D).

Sacral vertebrae. According to the condition in the holotype and LFGT-D0003 (Wang et al., 2017: Fig. 4), the sacrum of Xingxiulong consists of four sacral vertebrae; this feature currently represents a localized autapomorphy of Xingxiulong (Wang et al., 2017). Although only three sacral vertebrae are articulated in LFGT-D0001, the last element that is articulated with the dorsal series possesses a much wider diapophysis compared to that of the previous dorsal vertebra and is articulated with expanded ribs (Fig. 11), and thus this element is interpreted as the first sacral as opposed to the final dorsal. Given the morphology and relative position of the sacrum, the cranial-most sacral is interpreted as a dorsosacral, the middle two elements are primordial sacrals, and the caudal one is interpreted as a caudosacral.

In the holotype, the first sacral vertebra (dorsosacral) is situated medially between the cranial end of the pubic peduncle and the acetabulum of the ilium (Wang et al., 2017; Fig. 4A, C). This sacral is not fully fused to the subsequent element (first primordial sacral), with a clear demarcation between these two elements. Viewed ventrally, the centrum is more constricted transversely at its midpoint than in the other sacral centra. The centrum of the first sacral is similar in length to the presacral vertebrae and the last sacral vertebra (caudosacral) but longer than the centra of the two primordial sacrals. In LFGT-D0001, the diapophysis of the first sacral is short and sutured tightly to the sacral rib, which is a markedly expanded element that extends craniolaterally, although its articular surface with the ilium has been damaged (Fig. 11). The neural spine is higher than that of the presacral vertebrae, but its dorsal end is more similar in shape to that of the previous dorsals than the subsequent sacral elements, with a prominent laterally expanded dorsal table.

The second sacral vertebra in the holotype, which is the first primordial sacral, is located slightly cranial to the level of the ischial peduncle of the ilium (Wang et al., 2017; Fig. 4A,C). Ventrally, the centrum is obscured mostly by a fragment of the ilium, so more details cannot be ascertained. The second sacral centrum is fused with the third sacral centrum (the second primordial sacral), and these two elements share almost the same length. In dorsal view, the diapophysis is projected laterally and is the craniocaudally widest of all the sacral vertebrae. The sacral ribs of the second sacral vertebra are covered in the matrix and hence we cannot observe their features.

The third sacral vertebra (the second primordial sacral) is placed between the ischial peduncle and the postacetabular process of the ilium (Wang et al., 2017: Fig. 4A,C). The diapophysis is extended caudolaterally. In

Fig. 16. Caudal vertebrae 3–21 (LFGT-D0001) in (A) left lateral and (B) ventral views. Scale bar = 10 cm.

caudal view, the articular facet of the left sacral rib with the ilium is singular and nearly half as deep as the ilium.

The fourth sacral vertebra (caudosacral) is located at the level of the postacetabular process of the ilium, although its centrum projects beyond the caudal margin of the postacetabular process, which is possibly due to preservation (Wang et al., 2017: Fig. 4A,C). Although separated from the postacetabular process of the ilium by compression, in caudal view the sacral rib is fully fused to the transverse process and forms a lateral expansion that would have extended as far caudolaterally as that of the second primordial sacral to contact the ilium.

Caudal vertebrae. Nearly complete caudal vertebrae 1–35 and several articulated fragments are preserved in the holotype (Fig. 15, and also see Fig. S1B). A nearly articulated series of 19 caudal vertebrae is preserved in LFGT-D0001 (Fig. 16), and the first element of this series is interpreted as caudal 3 based on its morphology with respect to that of the holotype. The distal caudal vertebrae of both specimens are not preserved.

In the holotype, the length of the centrum is less than the height of the cranial and caudal articular surfaces (Fig. 15); the length/height ratios of caudal 1 at the cranial and caudal articular facets are 0.66 and 0.65, respectively. These values increase along the caudal series, with the length/height ratio of caudal 31 being 1.19. In LFGT-D0001, the length/height ratios of the proximal-most preserved caudal at the cranial and caudal articular facets are 0.68 and 0.74, respectively (Fig. 16), similar to that of the third centrum (0.71 and 0.7) in the holotype; hence, we interpret it as the third caudal vertebra. The lateral surfaces of the centra of the caudal vertebrae are concave. It is likely that all the caudal centra of the holotype have amphicoelous articular facets. In LFGT-D0001, the ventral surfaces of the centra of caudal 3 to caudal 7 possess broad longitudinal sulci (Fig. 16B), which are absent in the following caudals; this ventral sulcus is described as present on all the caudal centra except the two most proximal caudals in Lufengosaurus (Young, 1941a) and Yunnanosaurus (Young, 1942). The ventral surfaces of the proximal caudals (caudal 1–caudal 5) in the holotype, however, possess a wide ridge instead of a sulcus (Fig. 15C). The discrepancy between these two skeletons may represent individual or sexual dimorphism, or simply be a result of taphonomic flattening in the case of the holotype (see Discussion).

The neural arches are nearly complete in the caudal series. The right transverse processes are well developed, although the left elements are markedly shorter than the right ones due to deformation. The proximal transverse processes (caudals 1–12) are dorsolaterally directed, elongated and dorsoventrally flat, whereas the distal elements are slenderer and nearly horizontally directed. All the caudal transverse processes are situated on the neural arches; this condition is also present in other non-sauropodan sauropodomorphs, but in sauropods the transverse processes extend from the neural arches to the centra of the proximal caudal vertebrae. The prezygapophyses are projected cranially beyond the cranial edge of the centra. The postzygapophyses are placed higher than the prezygapophyses and extend beyond the caudal edge of the centra. The lamination of the caudal vertebrae is poorly developed; only the prezygodiapophyseal laminae are present in caudals 3–8 in LFGT-D0001. The neural spines are tall and caudodorsally directed. The base of the proximal neural spines is elongated, greater than half the length of the neural arch and slightly less than the length of the centra, which is consistent with the condition in most basal sauropodomorphs.

Ribs and chevrons. Some fragments of the cervical ribs and the dorsal ribs are preserved in all the three skeletons (Figs. 4, 5 and 8–13). The dorsal ribs are appressed to the dorsal vertebrae but not in their original articulation. The proximal end of the dorsal rib is Y-shaped, with both the capitulum and tuberculum preserved.

Fig. 17. Six isolated chevrons (LFGT-D0001) in proximal views. Scale bar = 10 cm.

Six isolated chevrons and three chevrons in articulation with the caudal vertebrae are preserved in D0001, which possibly represent the proximal elements (Fig. 17). Some proximal fragments of the chevrons are preserved in the holotype (Fig. 15). The chevrons are distinctively Y-shaped, with their cranial ends transversely bridged by a caudodorsally oriented, concave articular facet. The subtriangular haemal canal for the caudal blood vessels is situated under the articular facet. The distal blade is transversely flattened, with the distal ends of the chevrons slightly expanded transversely.

DISCUSSION

Based on the above description, the differential diagnoses of the axial skeleton of Xingxiulong chengi can be summarized as by the following features: (1) subcircular orbit (ventrally constricted in Jingshanosaurus (Zhang and Yang, 1995)); (2) position of the rostral margin of the infratemporal fenestra caudal to the orbit (also present in Plateosaurus (Prieto-Márquez and Norell, 2011); however, this margin extends under the caudal half of the orbit in Lufengosaurus (Barrett et al., 2005), Yunnanosaurus (Barrett et al., 2007), and Jingshanosaurus (Zhang and Yang, 1995)); (3) slender rostral process of the frontal intruding between the prefrontal and the nasal (also present in Plateosaurus (Prieto-Márquez and Norell, 2011), but absent in Lufengosaurus); (4) gently curved dorsal margin of postorbital in lateral view (also present in Plateosaurus (Prieto-Márquez and Norell, 2011) and Sarahsaurus [TMM 43646-2; Marsh and Rowe, 2018], but with a distinct embayment between the rostral and caudal dorsal processes in Lufengosaurus, Yunnanosaurus, Jingshanosaurus, and Massospondylus (Chapelle and Choiniere, 2018)); (5) angle of divergence between jugal and squamosal rami of quadratojugal close to 90 degrees (also present in Yunnanosaurus, Jingshanosaurus, and Massospondylus (Chapelle and Choiniere, 2018), but the two rami more close to parallel in Plateosaurus (Prieto-Márquez and Norell, 2011) and Lufengosaurus); (6) length of the jugal ramus of quadratojugal longer than the squamosal ramus (also present in Plateosaurus (Prieto-Márquez and Norell, 2011) and Massospondylus (Chapelle and Choiniere, 2018)); (7) postparietal fenestra between supraoccipital and parietals (also present in Plateosaurus (Prieto-Márquez and Norell, 2011), but absent in Yunnanosaurus and Jingshanosaurus); (8) erect to gently sloping supraoccipital plate (also present in Yunnanosaurus, Jingshanosaurus, and Massospondylus (Chapelle and Choiniere, 2018), but strongly sloping forward so that the dorsal tip lies level with the basipterygoid processes in Plateosaurus (Prieto-Márquez and Norell, 2011) and Lufengosaurus); (9) relatively straight floor of the braincase in lateral view with the basal tubera, basipterygoid processes and parasphenoid rostrum roughly aligned (bent with the basipterygoid processes and the parasphenoid rostrum below the level of the basioccipital condyle and the basal tubera in Plateosaurus (Prieto-Márquez and Norell, 2011) and Lufengosaurus, and bent with the basal tubera lowered below the level of the basioccipital and the parasphenoid rostrum raised above it in Jingshanosaurus); (10) position of jaw joint no lower than the level of the dorsal margin of the dentary (also present in Yunnanosaurus, but depressed, well below this level in Plateosaurus, Lufengosaurus, and Jingshanosaurus); (11) a stout, tab-like medial process of the articular behind the glenoid (also present in Jingshanosaurus, but absent in Lufengosaurus); (12) linearly placed teeth with crowns not overlapping (also present in Yunnanosaurus, but imbricated with distal side of tooth overlapping mesial side of the succeeding tooth in Plateosaurus (Prieto-Márquez and Norell, 2011), Lufengosaurus, Jingshanosaurus, and Massospondylus (Chapelle and Choiniere, 2018); (13) laterally

expanded neural spine table in caudal dorsal vertebrae (absent in Lufengosaurus, Yunnanosaurus, Jingshanosaurus, Plateosaurus [MB R 4430 skelett C], and Massospondylus (Chapelle and Choiniere, 2018)); (14) four sacral vertebrae (three sacral vertebrae present in Lufengosaurus, Yunnanosaurus, Jingshanosaurus, Plateosaurus (Moser, 2003), and Massospondylus (Chapelle and Choiniere, 2018)).

The skull of Xingxiulong displays several features that are more similar to those in non-massopodan (sensu Yates, 2007a, 2007b) or non-sauropodiform sauropodomorphs than in basal sauropodiforms based on the phylogenetic framework of Wang et al. (2017), for example: the lacrimal of Xingxiulong bears a prominent flange on the rostral margin, similar to that in Lufengosaurus, Adeopapposaurus and Massospondylus, but contrasts with Yunnanosaurus and Jingshanosaurus in which this flange is absent; the dorsal margin of the postorbital of Xingxiulong is only slightly concave, resembling that of some basal taxa such as Plateosaurus, but unlike the more derived taxa in which dorsal margin of postorbital is more curved (e.g., Lufengosaurus, Coloradisaurus, Adeopapposaurus, Jingshanosaurus, and Melanorosaurus [NM QR3314; Yates, 2007b]); the position of the rostral margin of the infratemporal fenestra of Xingxiulong is caudal to the orbit, similar to that in Plateosaurus, but this margin extends under the caudal half of the orbit in Lufengosaurus, Yunnanosaurus, and Jingshanosaurus; the basipterygoid processes of Xingxiulong are long, slender, and diverge from each other at an angle of approximately 80 degrees, shared with those of Plateosaurus, whereas in Lufengosaurus and Jingshanosaurus the basipterygoid processes are short, robust, and nearly parallel with each other.

The postcranial axial skeleton of Xingxiulong, however, possesses some interesting features. The possession of four sacral vertebrae has been discussed previously (e.g., Pol et al., 2011; Wang et al., 2017) as a relatively derived condition among basal sauropodomorphs. And two other distinctive or unique features should be mentioned: (1) Caudal dorsal vertebrae with laterally expanded neural spine tables. The 12th–14th dorsal vertebrae of Xingxiulong have laterally expanded neural spine tables, becoming more prominent from cranial to caudal (Fig. 11), which is considered as an autapomorphy (Wang et al., 2017). However, this feature was also reported in the recently described Yizhousaurus (Zhang et al., 2018). (2) Proximal caudal vertebrae with ventral ridges or sulci. As described above, the ventral surfaces of the proximal caudal centra of LFGT-D0001 display longitudinal sulci (Fig. 16B); however, in the holotype, the same region of the proximal caudal centra is occupied by a wide ridge (Fig. 15C). It should be noted that the ventral sulcus or flat ventral surface is commonly present in the proximal caudal vertebrae in non-sauropodan sauropodomorphs, but the presence of a ventral ridge on the proximal caudals is an uncommon feature among them. Eucnemesaurus entaxonis was also described to possess a similar ridge (although much more acute) and this feature was suggested as a possible autapomorphy of this taxon, albeit possibly exaggerated by compression (McPhee et al., 2015). Although taphonomic processes cannot be ruled out, the discrepancy present in the caudal vertebrae of Xingxiulong indicates possible dimorphism or individual plasticity within non-sauropodan sauropodomorphs that should be taken into account during future research on these taxa.

Finally, the appendicular skeleton of Xingxiulong possesses several derived features that generally typify derived non-sauropodan sauropodiforms, such as a robust scapula (e.g., Lessemsaurus (Pol and Powell, 2007b) and Antetonitrus (McPhee et al., 2014)) and a pubis with elongated pubic plate (Wang et al., 2017). We hope this study on the axial skeleton and ongoing work on the appendicular skeleton of Xingxiulong will contribute to future comparative and phylogenetic studies of non-sauropodan sauropodomorphs.

ACKNOWLEDGEMENTS

The authors thank Peter Dodson and Brandon Hedrick for inviting us to contribute to this special issue, and two anonymous reviewers for their valuable comments that improved the manuscript. We also appreciate Xiao-Chun Wu, Cecilia Apaldetti, and Alejandro Otero for their critical discussion and support, Wei Gao for taking all the photographs, and many other staffs of LFGZ and Institute of Vertebrate Paleontology and Paleoanthropology, Chinese Academy of Sciences for various supports.

LITERITURE CITED

Apaldetti C, Martinez RN, Pol D, Souter T. 2014. Redescription of the Skull of Coloradisaurus brevis (Dinosauria, Sauropodomorpha) from the Late Triassic Los Colorados Formation of the Ischigualasto-Villa Union Basin, northwestern Argentina. J Vertebr Paleontol 34:1113–1132.

Apaldetti C, Martínez RN, Cerda IA, Pol D, Alcober O. 2018. An early trend towards gigantism in Triassic sauropodomorph dinosaurs. Nat Ecol Evol 2:1227–1232. https://doi.org/10.1038/s41559-018-0599-y.

Barrett PM, Upchurch P, Wang X-L. 2005. Cranial osteology of Lufengosaurus huenei young (Dinosauria: Prosauropoda) from the Lower Jurassic of Yunnan, People's Republic of China. J Vertebr Paleontol 25:806–822.

Barrett PM, Upchurch P, Zhou X-D, Wang X-L. 2007. The skull of Yunnanosaurus huangi Young, 1942 (Dinosauria: Prosauropoda) from the Lower Lufeng Formation (Lower Jurassic) of Yunnan, China. Zool J Linn Soc 150:319–341.

Bronzati M, Rauhut OWM. 2018. Braincase redescription of Efraasia minor Huene, 1908 (Dinosauria: Sauropodomorpha) from the Late Triassic of Germany, with comments on the evolution of the sauropodomorph braincase. Zool J Linn Soc 182:173–224.

Brusatte SL, Nesbitt SJ, Irmis RB, Butler RJ, Benton MJ, Norell MA. 2010. The origin and early radiation of dinosaurs. Earth Sci Rev 101:68–100.

Chapelle KEJ, Choiniere JN. 2018. A revised cranial description of Massospondylus carinatus Owen (Dinosauria: Sauropodomorpha) based on computed tomographic scans and a review of cranial characters for basal Sauropodomorpha. PeerJ 6:e4224.

Cooper MR. 1981. The prosauropod dinosaur Massospondylus carinatus Owen from Zimbabwe: its biology, mode of life and phylogenetic significance. Nat Sci Ser B 6:689–840.

Langer MC. 2014. The origins of Dinosauria: much ado about nothing. Palaeontology 57:469–478.

Lü J-C, Kobayashi Y, Li T-G, Zhong S-M. 2010. A new basal sauropod dinosaur from the Lufeng Basin, Yunnan Province, southwestern China. Acta Geol Sin-Engl Ed 84:1336–1342.

Marsh AD, Rowe TB. 2018. Anatomy and systematics of the sauropodomorph Sarahsaurus aurifontanalis from the Early Jurassic Kayenta Formation. PLoS One 13:e0204007. https://doi.org/10.1371/journal.pone.0204007.

Martínez RN. 2009. Adeopapposaurus mognai, gen. et sp. nov. (Dinosauria: Sauropodomorpha), with comments on adaptations of basal Sauropodomorpha. J Vertebr Paleontol 29:142–164.

Mcphee BW, Choiniere JN. 2017. The osteology of Pulanesaura eocollum: implications for the inclusivity of Sauropoda (Dinosauria). Zool J Linn Soc 182:830–861. https://doi.org/10.1093/zoolinnean/zlx1074.

McPhee BW, Yates AM, Choiniere JN, Abdala F. 2014. The complete anatomy and phylogenetic relationships of Antetonitrus ingenipes (Sauropodiformes, Dinosauria): implications for the origins of Sauropoda. Zool J Linn Soc 171:151–205.

McPhee BW, Choiniere JN, Yates AM, Viglietti PA. 2015. A second species of Eucnemesaurus Van Hoepen, 1920 (Dinosauria, Sauropodomorpha): new information on the diversity and evolution of the sauropodomorph fauna of South Africa's lower Elliot Formation (latest Triassic). J Vertebr Paleontol 35:e980504.

McPhee BW, Bordy EM, Sciscio L, Choiniere JN. 2017. The sauropodomorph biostratigraphy of the Elliot Formation of southern Africa: tracking the evolution of Sauropodomorpha across the Triassic–Jurassic boundary. Acta Palaeontol Pol 62:441–465.

Moser M. 2003. Plateosaurus engelhardti Meyer, 1837 (Dinosauria, Sauropodomorpha) aus dem Feuerletten (Mittlekeuper; Obertrias) von Bayern. Zitteliana Reihe B 24:1–186.

Müller RT, Langer MC, Bronzati M, Pacheco CP, Cabreira SF, Dias-Da-Silva S. 2018. Early evolution of sauropodomorphs: anatomy and phylogenetic relationships of a remarkably well-preserved dinosaur from the Upper Triassic of southern Brazil. Biol Lett 14: 20180633. https://doi.org/10.1098/rsbl.2018.0633.

Padian K. 2013. The problem of dinosaur origins: integrating three approaches to the rise of Dinosauria. Earth Environ Sci Trans R Soc Edinburgh 103:1–20.

Pol D, Powell JE. 2007a. Skull anatomy of Mussaurus patagonicus (Dinosauria: Sauropodomorpha) from the Late Triassic of Patagonia. Hist Biol 19:125–144.

Pol D, Powell JE. 2007b. New information on Lessemsaurus sauropoides (Dinosauria: Sauropodomorpha) from the Upper Triassic of Argentina. In: Barrett PM, Batten DJ, editors. Evolution and palaeobiology of early sauropodomorph dinosaurs. Special papers in palaeontology, London, the Palaeontological Association Vol. 77. p 223–243.

Pol D, Garrido A, Cerda IA. 2011. A new sauropodomorph dinosaur from the Early Jurassic of Patagonia and the origin and evolution of the sauropod-type sacrum. PLoS One 6:e14572.

Pretto FA, Langer MC, Schultz CL. 2019. A new dinosaur (Saurischia: Sauropodomorpha) from the Late Triassic of Brazil provides insights on the evolution of sauropodomorph body plan. Zool J Linn Soc 185:388–416.

Prieto-Márquez A, Norell MA. 2011. Redescription of a nearly complete skull of Plateosaurus (Dinosauria: Sauropodomorpha) from the Late Triassic of Trossingen (Germany). Am Mus Novit 3727:1–58.

Regalado Fernandez OR, Upchurch P, Barrett PM, Mannion P, Maidment SCR. 2018. A reassessment of the phylogeny of basal sauropodomorphs through comparative cladistics and the supermatrix approach. In: Marzola M, Mateus O, Moreno-Azanza M, editors. Abstract book of the XVI Annual Meeting of the European Association of Vertebrate Palaeontology, Caparica, Portugal June 26th-July 1st, 2018.

Sekiya T. 2010. A new prosauropod dinosaur from Lower Jurassic in Lufeng of Yunnan. Global Geol 29:6–15.

Wang Y-M, You H-L, Wang T. 2017. A new basal sauropodiform dinosaur from the Lower Jurassic of Yunnan Province, China. Sci Rep 7:41881.

Wilson JA. 1999. A nomenclature for vertebral laminae in sauropods and other saurischian dinosaurs. J Vertebr Paleontol 19:639–653.

Yates AM. 2007a. Solving a dinosaurian puzzle: the identity of Aliwalia rex Galton. Hist Biol 19:93–123.

Yates AM. 2007b. The first complete skull of the Triassic dinosaur Melanorosaurus Haughton (Sauropodomorpha: Anchisauria). Spec Pap Paleontol 77:9–55.

Young C-C. 1941a. A complete osteology of Lufengosaurus hueni Young (gen. et sp. nov.) from Lufeng, Yunnan, China. Palaeontol Sin New Ser C 7:1–53.

Young C-C. 1941b. Gyposaurus sinensis Young. (sp. nov.), a new Prosauropoda from the Upper Triassic beds at Lufeng, Yunnan. Bull Geol Soc China 21:205–253.

Young C-C. 1942. Yunnanosaurus huangi Young (gen. et sp. nov.), a new Prosauropoda from the Red Beds at Lufeng, Yunnan. Bull Geol Soc China 22:63–104.

Young C-C. 1947. On Lufengosaurus magnus Young (sp. nov.) and additional finds of Lufengosaurus huenei Young. Palaeontol Sin New Ser C 12:1–53.

Young C-C. 1951. The Lufeng saurischian fauna in China. Palaeontol Sin New Ser C 13:1–94.

Zhang Y-H, Yang Z-L. 1995. A new complete osteology of Prosauropoda in Lufeng Basin, Yunnan, China: Jingshanosaurus. Kunming: Yunnan Publishing House of Science and Technology.

Zhang Q-N, You H-L, Wang T, Chatterjee S. 2018. A new sauropodiform dinosaur with a 'sauropodan' skull from the Lower Jurassic Lufeng Formation of Yunnan Province, China. Sci Rep 8:13464.